の想起（以下ネガティブ情動想起）の2種類のタスクをそれぞれ3分間行い，ポジティブ情動想起タスクではこれまでの人生で最も嬉しかったことを，ネガティブ情動想起では最も悲しかったことを想起するよう指示した．役割演技タスクは，ポジティブな内容（以下ポジティブ役割演技）・ネガティブな内容（以下ネガティブ役割演技）の2種類のセリフを用いて，座位のままで声のみの役割演技をそれぞれ3分間行った．被験者に対して，ポジティブ役割演技の際には嬉しい・楽しいなどの気持ちを存分にこめて読むように，ネガティブ役割演技の際には悲しい・悔しいなどの気持ちを存分にこめて読むようにとそれぞれ伝えた．セリフは，ポジティブ役割演技タスクでは『アルプスの少女ハイジ』（ズイヨー映像），ネガティブ役割演技タスクでは『フランダースの犬』（日本アニメーション）を用いた．順序による影響を排除するために，被験者ごとにセリフや想起のポジティブ・ネガティブの順序を入れ替えた．

これら4種類のタスクをそれぞれ前後に安静（3分間）を取りながら連続して行い，その間継続的に，左右前頭葉の酸素化ヘモグロビン（以下O2Hb）濃度を近赤外線酸素モニター（Near infrared spectroscopy, NIRO200，浜松ホトニクス社，以下NIRS）を用いて既報の方法に基づき測定した17)．今回は左右の前額部に照射プローブ及び検出プローブを装着し，左右前頭葉におけるO2Hb濃度の相対的な変化量を測定することによってタスク中の前頭葉の活性の変化を推測した．プローブは両面シールを用いて固定し，アーティファクトを避けるためにプローブの上から黒色布を巻いて太陽光を遮断した．基準値は安静時最終30秒間の平均値を0に補正して用い，タスクを行った際の前頭葉の相対的血流変化を1秒ごとに算出した．

また，それぞれのタスク中と前後の安静時間には，自律神経バランス分析加速度脈波計を用いて心拍，及び交感神経／副交感神経比を測定した．自律神経バランス分析加速度脈波計（Pulse Analyzer Plus ; TAS9，YKC社）を用いた．座位でセンサーを左示指に装着し，測定時間を2分30秒間としてそれぞれの値を1秒ごとに測定し，平均値を算出した．得られたデータは，SPSSソフトを使って統計解析を行った．

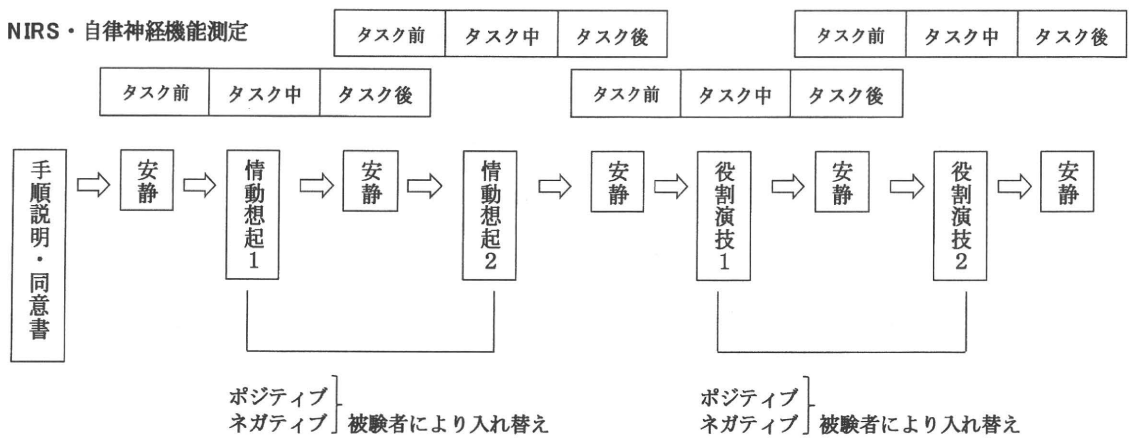

Figure 1.　実験1の手順

実験1で用いた手順を図に示す．すべての被験者に対し情動想起二種類（ポジティブ・ネガティブ），及び役割演技二種類（ポジティブ・ネガティブ）のタスクを安静を前後に挟み行った．それぞれのタスク内の順番は順番による影響を考慮し，被験者ごとに入れ替えた．タスクの前後の安静をそれぞれ「タスク前」「タスク後」，タスク施行中を「タスク中」とし，この間のNIRS・自律神経機能測定結果から被験者における平均値を求め，グラフ化と統計処理を行った．

3．結果

情動想起および役割演技タスクを行った際の，19名の健常被験者における前頭葉O2Hb濃度相対値の測定結果の平均値をFigure 2に示した．情動想起タスクにおいては，ポジティブ情動想起（Figure2A）・ネガティブ情動想起（Figure2B）ともに，タスク開始から終了にかけてO2Hb濃度の経時的な増大が見られた．これらはいずれも，左側優位に増加する傾向が見られた．

一方役割演技タスクにおいてもやはり，ポジティブ（Figure2C）・ネガティブ（Figure2D）役割演技のいずれにおいても，O2Hb濃度は安静時と比べタスク開始と共にわずかに上昇する傾向を示した．また，わずかに左側優位傾向であり，O2Hb濃度増大の持続時間は情動想起に比較して短い傾向が観察された．

情動想起タスク及び役割演技タスクを行った際及びその前後の安静時の，19名の健常被験者における心拍と交感神経／副交感神経比の測定結果の平均値をFigure 3に示した．

心拍においては，情動想起，役割演技ともに，ポジティブ・ネガティブすべてのタスクにおいて，タスク中に上昇し，タスク後に下降する傾向がみられた（Figure3A）．ポジティブ情動想起タスクでは，70.2+/-9.2→74.6+/-9.8→70.2+/-9.6回/分(タスク前平均+/-標準偏差→タスク中平均+/-標準偏差→タスク後平均+/-標準偏差，以下同じ)，ネガティブ情動想起タスクでは69.6+/-7.8→73.9+/-9.6→69.3+/-9.0回/分と変化した．また，ポジティブ役割演技タスクにおいては69.8+/-9.5→77.3+/-9.3→70.6+/-9.6回/分，ネガティブ役割演技タスクでは70.7+/-9.4→74.9+/-9.3→70.3+/-9.2回/分と変化して

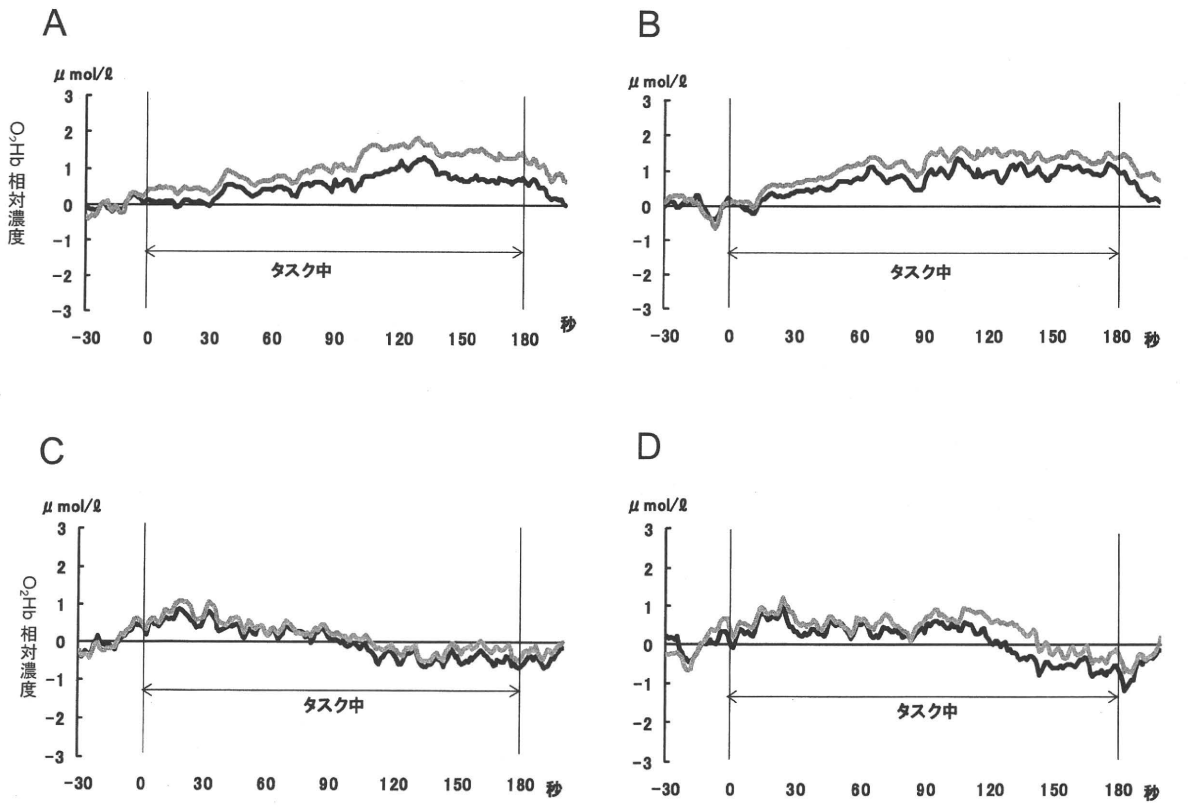

Figure 2.　情動想起・役割演技タスク遂行時の前頭葉02Hb濃度変化（健常成人19名平均）

——右側　——左側における，A．ポジティブ情動想起，B．ネガティブ情動想起，C．ポジティブ役割演技，D．ネガティブ役割演技，のそれぞれのタスク遂行による前頭葉02Hb濃度の相対変化をグラフで表した．矢印はタスク遂行時間を表す．

おり，すべてのタスクの前—中，中—後の比較において，Wilcoxonの符号付き順位検定で有意差が検出された（Figure3A参照）．

一方，交感神経／副交感神経比においても，情動想起，役割演技ともにポジティブ・ネガティブすべてのタスクにおいて，タスク中の上昇する傾向，すなわち交感神経優位に転じる傾向がみられた（Figure3B）．ポジティブ情動想起タスクでは，1.156+/-0.027→1.178+/-0.031→1.162+/-0.038回/分(タスク前平均+/-標準誤差→タスク中平均+/-標準誤差→タスク後平均+/-標準誤差，以下同じ)，ネガティブ情動想起タスクでは1.163+/-0.039→1.176+/-0.024→1.159+/-0.033回/分と変化した．また，ポジティブ役割演技タスクにおいては1.171+/-0.039→1.176+/-0.044→1.170+/-0.041回/分，ネガティブ役割演技タスクでは1.167+/-0.037→1.182+/-0.039→1.171+/-0.038回/分と変化しており，このうちWilcoxonの符号付き順位検定で有意差が検出されたのは，ポジティブ情動想起のタスク前-タスク中，タスク中 - タスク後，ネガティブ情動想起のタスク中 - タスク後，及びネガティブ役割演技のタスク前 - タスク中の比較においてであった．

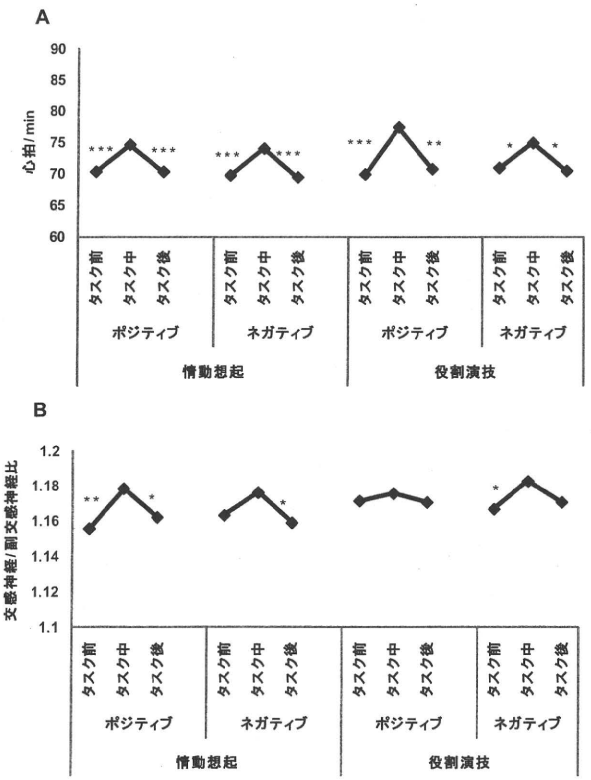

Figure 3.　情動想起・役割演技タスク遂行時の自律神経機能変化（健常成人19名平均）

それぞれのタスク遂行前・中・後に測定した心拍(A)，交感神経／副交感神経比(B)の変化をグラフで表した．Wilcoxonの符号付き順位和検定により有意差が認められた箇所を示した(* p<0.05, ** p<0.005, *** p<0.001)．

実験 2

1．対象

対象は実験に関して十分な説明を行い，学校長及びクラス担任教員より実施の承諾を得られた，S県某市のX小学校である．そのうち4学年の一学級の児童37名（男子18名，女子19名：平均年齢9.6歳）を対象とした．

2．方法

実験は2009年10月下旬から11月中旬にかけて，X小学校4学年の教室で行った．

全5回にわたり，授業時間を利用して，クラスの全児童に対し，ポジティブな内容とネガティブな内容の2種類のセリフを用いた音読のみの役割演技タスクを一回ずつ行わせた．セリフは，実験1で用いた『アルプスの少女ハイジ』(ズイヨー映像)及び『フランダースの犬』（日本アニメーション）の抜粋を，さらに児童用に修正(ふりがなを振る，字を大きくするなど）し用いた．順序による影響を排除するために，各回でタスクの順序を入れ替えた．また，37名の児童による一斉読みをするという方法をとったため，演技に集中できるよう他の児童と読む速度や読み方を合わせなくても良いということを事前に児童に伝えた．

それぞれの回のタスク前に，心身に関する質問20項目からなる質問紙（巻末参考資料）を用いた不定愁訴に関わると考えられる自覚所見の調査を行った．

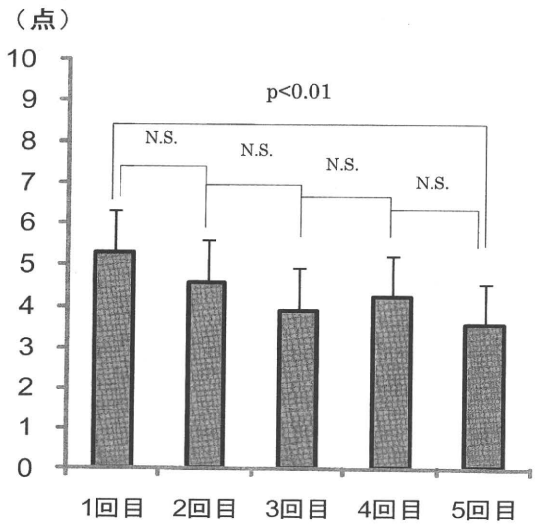

Figure 4.　役割演技実践に伴う
児童の不定愁訴得点の5回の推移（n=24）

5回の役割演技実践を行う際に行った，不定愁訴質問紙の得点の平均値および標準偏差をグラフに表した．各回間では有意差は認めなかったが（N.S; not significant）1回目-5回目間でp<0.01の有意差を認めた（Wilcoxonの符号付き順位検定による）

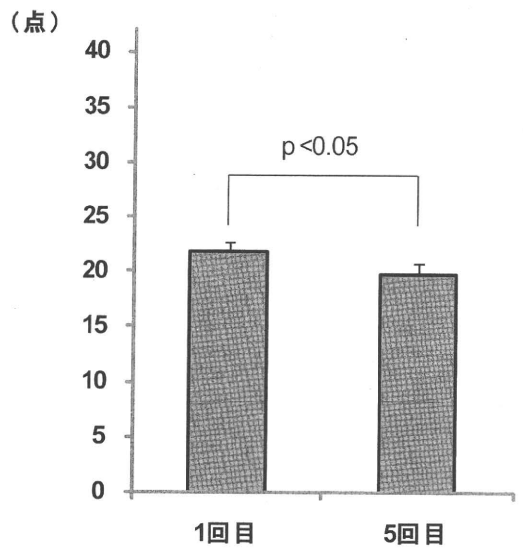

Figure 5.　役割演技実践の前後における
児童のCMAS得点の変化（n=34）

5回の役割演技実践を通して，児童のCMAS得点平均値は役割演技実践1回目と比較して5回目で有意に減少した（p<0.05；Wilcoxonの符号付き順位検定による）

また，実践1回目と5回目には，日本版Children's Manifest Anxiety Scale（以下CMAS；三京書房）を用いて児童の有する不安の測定を行った[18]．

使用した質問紙は予め番号をふったもの全5回分を封筒に入れ，この封筒を初回調査時に被験者にランダムに渡して実施し，検査者が被験者を番号で特定できないように配慮した．実験終了後に封筒内のデータを比較検討することにより，無記名連結データとして処理を行った．調査票には性別と年齢のみを記載させた．

3．結果

実践に参加した全児童37名のうち，役割演技の実践授業の開始前に行った不定愁訴質問紙を，5回分すべて記入した児童24名（平均9.58歳）について，それぞれの役割演技実践前における不定愁訴得点の平均値を計算し，Figure 4に示した．1回目の調査における平均得点は5.29+/-0.67（平均+/-標準誤差，以下同じ），2回目4.58+/-0.69，3回目3.92+/-0.62，4回目4.21+/-0.71，5回目3.54+/-0.62であり，初回と比較して最終回では平均値が有意に減少していた（p<0.01；Wilcoxonの符号付き順位検定による）．男女差は見られなかった．

また，全児童37名中5回の役割演技実践の1回目及び5回目におけるCMAS質問紙をいずれも記入した34名（平均9.59歳）について集計した得点平均値をFigure 5 に示した．1回目においては平均得点21.7+/-1.48（平均+/-標準誤差，以下同じ），5回目では平均得点19.7+/-1.69であり，有意な減少がみられた（p<0.05；Wilcoxonの符号付き順位検定による）．男女による得点の差は見られなかった．

考察

今回，情動想起及び役割演技タスク中の前頭葉O2Hb濃度変化を検索した結果，健常群ではポジティブ及びネガティブ情動想起タスクを行った際に，タスクとともに左側優位の前頭葉血流内O2Hb濃度相対値の経時的な上昇が観察された（Figure 2A,B）．　情動想起タスクを施行し，イメージン

グ手法を用いて脳の片側優位性を測定した実験結果においては，左側優位の扁桃体－前頭葉系の活性化が起こる健常個体が大多数を占めることが繰り返し報告されている[9, 19]．このことから，今回設定した被験者は健常群として妥当な被験者群である考えられる．

また，健常者において文章を音読ないし黙読させるタスクを施行した際にNIRSで測定した前頭葉血流内O2Hb濃度は，上昇ではなくむしろ相対的低下を認めることが知られている[20, 21]．今回用いた，セリフを感情をこめて朗読する役割演技タスクは，健常被験者において平均的にタスク開始と共に前頭葉O2Hb濃度を上昇させる結果が得られたため，通常の音読とは異なり，情動想起に近い効果を与える負荷であったと推測される．

また，自律神経機能の変化においても，役割演技タスクの前・中・後の心拍及び交感神経／副交感神経比の変化の測定においては（Figure3B），情動想起タスクのそれ（Figure3A）と極めて類似した結果が得られており，心拍ではポジティブ・ネガティブとも前後と比較してタスク中に有意に上昇し，交感神経優位傾向に変化する傾向が観察された．

以上の結果より，役割演技タスクを行った際の前頭葉及び自律神経機能の変化には情動想起タスクを行った際のそれに類似する点を多く認め，役割演技を疑似情動想起刺激の一つとして捉えることが可能であることが示唆された．

健常成人では，情動などのストレス刺激により前頭葉左側が有意に活性化することが多いことが知られるが[9, 19]，一方で同様の刺激で右側を優位に活性化する個体も少数存在する．右側優位の活性化が認められる個体では，自律神経機能の脆弱性[9]やワクチンに対する免疫機能の相対的な低下[10]，さらには皮膚の炎症，湿疹の出現頻度が高いこと[11]などが報告されている．前頭葉から視床下部及び自律神経中枢への下行性のニューロンの存在や，情動と前頭葉，そして自律神経系の密接な関連，そして不安を制御するセロトニン神経系も良く知られていて[11, 22, 23]，これらセロトニン神経系や前頭葉機能は9~15歳までに外界からの刺激に呼応して可塑性を用いたシナプスの統合を行うことで成熟した形態へと発達していくため[12-14]，このような前頭葉レベルでのストレス耐性も，生後個体の受ける刺激に応じて獲得されるものであると推察される．

従って，学級活動において児童に繰り返す演技訓練による疑似情動刺激を行い，前頭葉や自律神経機能を初めとする様々な脳機能を刺激することでこれら機能の健常な発達を促すことは，ストレス耐性の獲得という観点で意義があると考えられる．

今回小学校児童に対し，5回の役割演技実践を行い測定した不定愁訴質問紙の合計得点とCMASによる不安得点において，児童の平均値がいずれも1回目と比較して5回目に有意に減少する結果が得られた（Figure 4，5）．約3週間の期間をかけての実践であり，その間に行われた学級活動・学校行事等による影響や児童の質問紙に対する馴れの効果による要因も，もちろん無視はできないであろう．しかしながら，実験1で示唆されたように，役割演技には前頭葉機能と自律神経機能変化を惹起する機能があることを考慮すれば，5回にわたる脳機能への繰り返しの刺激が，結果として児童の不安・不定愁訴を軽減させる，すなわちストレス耐性を変化させる効果を与える一因となったと考えることは妥当であろう．

以上より，不安や不定愁訴，そして関連する前頭葉機能としてのストレス耐性の改善・発達を期待できる役割演技を学級の活動の一環として取り入れることは，思春期以降の不定愁訴や不安を原因とする不登校をはじめとする様々な心身症状の発現を減少・軽減させる効果が期待できることが示唆され，非侵襲的な介入の方法として学級内で役割演技を継続的に行う意義はあると思われた．

演劇をすることによる直接的な効果についてはこれまであまり研究がなされていなかったが，これには演劇というものの総合性，つまり表現・発

声によるカタルシス，役割演技，セリフなどの暗記，全身運動，集団活動による協調などといった様々な要素が盛り込まれているという点が，原因のひとつとして考えられる．今回使用したNIRSは脳血流の変動を連続的に観察することが可能であり近年医療分野で応用されているが[24]，実験時の可動性に制限があるため座位による声のみの役割演技実験を一人ずつ行う形になり，また観客のいない空間でセリフを見ながら演技を行ったことによって，「演劇」の中から暗記や全身運動，集団意識などの要素を除外し，役割演技時の情動想起・思考・処理過程に焦点を当てることが可能になり，他の集団表現活動には見られない役割演技独自の効果が示唆されたといえる．ただし今回の実験では発声の要素が除外されておらず，役割演技の持つカタルシス効果を除外した実験を行うことができなかったため，今回得られた結果は役割演技中の想起・思考・処理過程に限定された効果であると断言することはできない．

また，成人において役割演技を繰り返し行った際の詳しい前頭葉機能，及び自律神経機能の測定が十分でなかったため，長期継続による脳機能への影響についての証明にまでは至っていない．今後は今回の研究結果を基盤として，タスク内容や実験前の統制条件を再度見直し，長期的な効果についてもさらに基礎実験と実践を行うことにより，学級活動への役割演技の普遍的な応用に向けて検証を重ねる必要があると考える．

謝辞

本研究を実施するにあたりご協力いただいた被験者，学校関係者，児童の皆様に深謝しここに記す．

【引用・参考文献】

1）Tomoda, A., Miike, T., Yonamine, K., Adachi,K., & Shiraishi, S. Disturbed circadian core body temperature rhythm and sleep disturbance in school refusal children and adolescents. *Biological Psychiatry*, 41, (1997) 810-13.

2）文部科学省 (2009). 平成20年度 文部科学白書 佐伯印刷

3）文部科学省 (2008.8). 平成19年度 児童生徒の問題行動等生徒指導上の諸問題に関する調査 http://www.mext.go.jp/b_menu/houdou/21/08/__icsFiles/afieldfile/2009/08/06/1282877_1_1.pdf (2010/04/07取得)

4）作田亮一・田副眞美・成田奈緒子　不定愁訴を有する不登校児の抱える「不安感」 —State-Trait Anxiety Inventoryによる心理学的評価およびSSRIの有効性— 脳と発達, 35, (2003) 394-400.

5）有田秀穂 (2006). 脳内物質のシステム神経生理学 —精神精気のニューロサイエンス— 中外医学社

6）Johnson, P. L., Lightman, S. L., & Lowry, C.A. A functional subset of serotonergic neurons in the rat ventrolateral periaqueductal gray implicated in the inhibition of sympathoexcitation and panic. *Annals of the New York Academy of Sciences*, 1018, (2004) 58-64.

7）Calogero, A. E., Bagdy, G., Szemeredi, K., Tartaglia, M. E., Gold, P. W., & Chrousos, G. P. Mechanisms of Serotonin Receptor Agonist-Induced Activation of the Hypothalamic-Pituitary-Adrenal Axis in the Rat. *Endocrinology*, 126, (1990) 1888-1894.

8）吉川裕子・永田純代・興梠文美　不登校児の現状 —前頭葉機能との関連について—　日本小児科学会雑誌, 99, (1995)2109-2115

9）Rosenkranz, M. A., Jackson, D. C., Dalton, K. M, Dolski, I., Ryff, C. D., Singer, B. H., Daniel Muller, D., Kalin, N. H., & Davidson, R. J. Affective style and in vivo immune response：Neurobehavioral mechanism. *Proceedings of the National Academy of Sciences of the United States of America*, 100, (2003) 11148 -11152.

10）Wang, J., Rao, H., Wetmore, S., Furlan, P. M., Korczykowski, M., †§, David F. Dinges, D. F., & Detre, J. A. Perfusion functional MRI reveals cerebral blood flow pattern under psychological stress. *Proceedings of the National Academy of Sciences of the United States of America*, 102, (2005) 17804-17809.

11）Tanida, M., Sakatani, K., Takano, R., & Tagai, K. Relation between asymmetry of prefrontal cortex activities and the autonomic nervous system during a mental arithmetic task : near infrared spectroscopy study. *Neuroscience Letters*, 369, (2004) 69-74.

12）Chugani, D.C., Muzik, O., Behen, M., Rothermel, R.,

Janisse, J. J., Lee, J., & Chugani, H. T. Developmental changes in brain serotonin synthesis capacity in autistic and nonautistic children. *Annals of neurology*, 45 (1999) 287-95.

13) Durston, S., Davidson, M. C., Tottenham, N., Galvan, A., Spicer, J., Fossella, J. A., & Casey, B. J. A shift from diffuse to focal cortical activity with development. *Developmental Sciences* , 9, (2006) 1-20.

14) Buckner, R. L., Andrews-Hanna, J. R., & Schagter, D. L. The brain's default network. Anatomy, function, and relevance to disease. *Annals of the New York Academy of Sciences*, 1124, (2008) 1-38.

15) 外林大作, 千葉ロール・プレイング研究会 (1981). 教育の現場におけるロール・プレイングの手引 誠信書房

16) 冨田博之 (1974). 現代演劇教育論 日本演劇教育連盟

17) Sakatani, K., Yamashita, D., Yamanaka, T., Oda, M., Yamashita, Y., Hoshino, T., Fujiwara, N. Murata,Y., & Katayama, Y. Changes of cerebral blood oxygenation and optical pathlength during activation and deactivation in the prefrontal cortex measured by time-resolved near infrared spectroscopy. *Life Sciences*, 78, (2006) 2734 -2741.

18) Castaneda, A., McCandless, B. R., & Palermo, D.S. The Children's Form of the Manifest Anxiety Scale. *Child Development*, 27, (1956) 317-326.

19) Baas, D., Aleman, A., Kahn, & Kahn, R. S. Lateralization of amygdala activation: a systematic review of functional neuroimaging studies. *Brain research. Brain research reviews*, 45, (2004) 96-103.

20) Fallgatter, A. J., Muller, T. J., & Strik, W. K. Prefrontal hypooxygenation during language processing assessed with near-infrared spectroscopy. *Neuropsychobiology*, 37, (1998)215-218.

21) Kuwabata, H., Kasai, K., Takizawa,R., Kawakubo, Y., Yamasue, H., Rogers, M. A., Ishijima, M ., Watanabe, K., & Kato,N. Decreased prefrontal activation during letter fluency task in adults with pervasive developmental disorders : a near-infrared spectroscopy study. *Behavioural brain research*, 172, (2006) 272-277.

22) Davidson, R.J., & Irwin, W. The functional neuroanatomy of emotion and affective style. *Trends in Cognive Sciences*, 3, (1999) 11-21.

23) Fischer, H., Andersson, J.L., Furmark, T., Wik, G., & Fredrikson, M. Right-sided human prefrontal brain activation during acquisition *of conditioned fear. Emotion* , 2, (2002) 233-241.

24) 伊藤宏樹・平山正昭・古池保雄 神経不全症患者の起立性低血圧時脳血流自動調節能—近赤外線分光法による検討— 臨床脳波, 47, (2005) 629-632.

昨日から今日のあなた自身について，はい か いいえ に　○をつけましょう.

1. 朝，すっきり起きられた（　はい　・　いいえ　）
2. 頭がいたくなった，いたい（　はい　・　いいえ　）
3. おなかがいたくなった，いたい（　はい　・　いいえ　）
4. 元気だ（　はい　・　いいえ　）
5. 肩こりがあった，ある（　はい　・　いいえ　）
6. 食欲がでなかった，ない（　はい　・　いいえ　）
7. 体がだるくなった，だるい（　はい　・　いいえ　）
8. 昼間でもねむかった，ねむい（　はい　・　いいえ　）
9. ご飯がおいしく食べられた（　はい　・　いいえ　）
10. 夜，なかなかねむれなかった（　はい　・　いいえ　）
11. 自分は人の役に立っていると思う（　はい　・　いいえ　）
12. わたしなんかいないほうがよいと思う（　はい　・　いいえ　）
13. やればできると思う（　はい　・　いいえ　）
14. イライラする（　はい　・　いいえ　）
15. やる気がしない（　はい　・　いいえ　）
16. 学校は楽しいと思う（　はい　・　いいえ　）
17. 人と話すのはいやだ（　はい　・　いいえ　）
18. 家は楽しいと思う（　はい　・　いいえ　）
19. 困ったことや心配なことを話せる人がいる（　はい　・　いいえ　）
20. 自分のことが好きだ（　はい　・　いいえ　）

巻末参考資料

実験2で用いた不定愁訴に関する質問項目を示す.

採点は，2, 3, 5, 6, 7, 8, 10, 14, 15, 17については，はいを1点，いいえを0点とし，1, 4, 9, 11, 12, 13, 16, 18, 19, 20については，はいを0点，いいえを1点として，全問の合計得点を出した.

Journal of Neuroscience Research

Journal of Neuroscience Research 88:2911–2922 (2010)

Analysis of Gene Expression Changes Associated With Long-Lasting Synaptic Enhancement in Hippocampal Slice Cultures After Repetitive Exposures to Glutamate

**Katsuhiro Kawaai,[1] Keiko Tominaga-Yoshino,[2] Tomoyoshi Urakubo,[2] Naoko Taniguchi,[2] Yasumitsu Kondoh,[3] Hideo Tashiro,[3] Akihiko Ogura,[2] and Tomoko Tashiro[1]*

[1]Department of Chemistry and Biological Science, School of Science and Engineering, Aoyama Gakuin University, Kanagawa, Japan
[2]Osaka University Graduate School of Frontier Biosciences and Osaka University Graduate School of Science, Osaka, Japan
[3]Probing Technology Laboratory, Discovery Research Institute, RIKEN, Wako, Saitama, Japan

We have previously shown that repetitive exposures to glutamate (100 μM, 3 min, three times at 24-hr intervals) induced a long-lasting synaptic enhancement accompanied by synaptogenesis in rat hippocampal slice cultures, a phenomenon termed *RISE* (for repetitive LTP-induced synaptic enhancement). To investigate the molecular mechanisms underlying RISE, we first analyzed the time course of gene expression changes between 4 hr and 12 days after repetitive stimulation using an original oligonucleotide microarray: "synaptoarray." The results demonstrated that changes in the expression of synapse-related genes were induced in two time phases, an early phase of 24–96 hr and a late phase of 6–12 days after the third stimulation. Comprehensive screening at 48 hr after the third stimulation using commercially available high-density microarrays provided candidate genes responsible for RISE. From real-time PCR analysis of these and related genes, two categories of genes were identified, 1) genes previously reported to be induced by physiological as well as epileptic activity (*bdnf, grm5, rgs2, syt4, ania4/carp/dclk*) and 2) genes involved in cofilin-based regulation of actin filament dynamics (*ywhaz, ssh1l, pak4, limk1, cfl*). In the first category, synaptotagmin 4 showed a third stimulation-specific up-regulation also at the protein level. Five genes in the second category were coordinately up-regulated by the second stimulation, resulting in a decrease in cofilin phosphorylation and an enhancement of actin filament dynamics. In contrast, after the third stimulation, they were differentially regulated to increase cofilin phosphorylation and enhance actin polymerization, which may be a key step leading to the establishment of RISE.

Key words: long-term potentiation; long-lasting plasticity; synaptogenesis; DNA microarray; repetitive stimulation

We can discriminate at least two phases in memory, short-term memory, which endures for a few hours, and long-term memory, which persists for several days and often much longer (Bear et al., 2001). Short-lasting synaptic plasticity, the presumed cellular basis of short-term memory, is thought to be accomplished by the rapid modification of synaptic strength in existing synapses (Lisman et al., 2002; Collingridge et al., 2004), whereas long-lasting synaptic plasticity representing long-term memory is associated with gene expression, de novo protein synthesis, and formation of new synaptic connections (Steward and Schuman, 2001; Lynch, 2004). Consistent with this idea, protein synthesis inhibitors can block the late-phase of long-term potentiation

Additional Supporting Information may be found in the online version of this article.

Katsuhiro Kawaai's current address is Calcium Oscillation Project, International Cooperative Research Project—Solution Oriented Research for Science and Technology, Japan Science and Technology Agency, 2-1 Hirosawa, Wako, Saitama 351-0198, Japan

Contract grant sponsor: High-Tech Research Center Project for Private Universities; Contract grant number: 20310037 (to T.T.); Contract grant sponsor: Ministry of Education, Culture, Sports, Science and Technology (MEXT) of the Japanese Government; Contract grant number: 19300108 (to A.O.); Contract grant sponsor: Ministry of Health, Labour and Welfare of the Japanese Government (to T.T.).

*Correspondence to: Tomoko Tashiro, Department of Chemistry and Biological Science, School of Science and Engineering, Aoyama Gakuin University, 5-10-1 Fuchinobe, Chuo-ku, Sagamihara, Kanagawa 252-5258, Japan. E-mail: ttashiro@aoyamagakuin.jp

Received 17 February 2010; Revised 29 April 2010; Accepted 12 May 2010

Published online 21 June 2010 in Wiley Online Library (wileyonlinelibrary.com). DOI: 10.1002/jnr.22457

(L-LTP) but leave the early-phase LTP (E-LTP) unaffected (Otani et al., 1989; Frey et al., 1996). Although several studies have reported that synaptic activities modulated transcription (Klann and Dever, 2004), the molecular mechanism underlying the conversion from the short-lasting plasticity to the long-lasting one remains poorly understood, mainly because of the lack of good model systems that allow the prolonged examination of synapse formation.

With cultured rat hippocampal slices, we have previously shown that repetitive exposures to glutamate (100 μM, 3 min, three times at 24-hr intervals) or repetitive protein kinase A (PKA) activation (forskolin, 50 μM, 3 min, three times at 24-hr intervals) induced an enhancement of excitatory postsynaptic potential (EPSP) coupled with synaptogenesis that lasted for more than 3 weeks (Tominaga-Yoshino et al., 2002, 2008; Shinoda et al., 2003; Urakubo et al., 2006). Although similar glutamate exposure or PKA activation once or twice produced L-LTP accompanied by acute morphological changes, it lasted for less than 24 hr. We thus concluded that more than three repetitions of the stimulation for LTP at appropriate intervals (3–24 hr) was necessary for the conversion of short-lasting enhancement into a long-lasting one (i.e., lasting for weeks) coupled with synaptogenesis. To distinguish this repetitive L-LTP-induced synaptic enhancement from the conventional single LTP, we named this phenomenon *RISE* (repetitive LTP-induced synaptic enhancement) in previous reports (Tominaga-Yoshino et al., 2002, 2008). The RISE in cultured hippocampal slices provides us with a good model with which to investigate the molecular mechanisms of conversion from the short-lasting plasticity to the long-lasting one.

Various studies have shown that experimental stimuli inducing L-LTP were accompanied by de novo transcription and translation of genes related to synaptic plasticity (Otani et al., 1989; Frey et al., 1996; Lynch, 2004). Because RISE was accompanied by an increase in the number of morphologically identifiable synaptic sites, we first analyzed the time course of gene expression changes after repetitive stimulation to elucidate the essential time window of synaptogenesis involved in this phenomenon. For this purpose, we used our original microarray, "synaptoarray," focused on 295 genes involved mainly in synaptic structure and function (Takahashi et al., 2005), which was capable of monitoring synaptogenesis in the developing cerebellum in vivo (Takahashi et al., 2005) as well as synaptic activity-dependent gene expression changes accompanying tetrodotoxin application in cultured neurons (Kitamura et al., 2007). The results revealed that dynamic changes in gene expression induced by repetitive glutamate stimulation were composed of two time phases, an early phase of 24–96 hr and a late phase of 6–12 days after the last stimulation.

Given these results, we carried out a comprehensive screening with high-density arrays 48 hr after the third stimulation. With several candidate genes selected from microarray data and related genes, up-regulation by repetitive stimulation was confirmed by real-time PCR, resulting in the identification of pathways responsible for the development of long-lasting synaptic plasticity.

MATERIALS AND METHODS

Slice Culture of the Rat Hippocampus and Glutamate Treatment

Hippocampal slices from Wistar/ST rat pups at postnatal day 8 (Nihon SLC, Shizuoka, Japan) were cultured as described previously (Tominaga-Yoshino et al., 2008). Before we began the stimulation experiments, the cultures were maintained at 34°C in humidified air for 12 days with medium renewal twice per week, during which time the slices became stabilized both physically and physiologically (Muller et al., 1993; Gahwiler et al., 1997). All animal treatments have been approved by the animal experimentation committees of Aoyama Gakuin and Osaka Universities. They were carried out under veterinary supervision and in accordance with the *Guidelines for the use of animals in neuroscience research* (Society for Neuroscience, 1992). Glutamate-exposure to induce LTP was carried out following the protocol described previously (Tominaga-Yoshino et al., 2008). The glutamate solution for stimulation (Glu solution) contained 100 μM glutamate in K^+-elevated, Mg^{2+}-free, HEPES-buffered balanced salt solution (15K HBSS; composed of 120.4 mM NaCl, 15 mM KCl, 5.5 mM glucose, 3 mM $CaCl_2$, 10 mM Hepes-NaOH, pH 7.4). Mock stimulation solution was composed of HBSS with low KCl concentration (5K BSS; composed of 130 mM NaCl, 5.4 mM KCl, 5.5 mM glucose, 1.26 mM $CaCl_2$, 0.8 mM $MgCl_2$, 10 mM HEPES-NaOH, pH 7.4). Healthy slices (judged from opacity) were exposed to Glu solution or mock stimulation solution for 3 min at 34°C each time. As shown in Figure 1, glutamate exposure was repeated three times at 24-hr intervals starting on day 12 in vitro (DIV 12) for the three times glutamate-stimulated ([3G]) series. Slices for the twice-stimulated ([2G]) series were exposed first to mock stimulation solution and then twice to Glu solution at 24-hr intervals each. Control slices were exposed three times to mock stimulation solution. Thirty similarly treated slices were used at each time point for RNA extraction.

Histological Evaluation of Cell Viability

Apoptotic cells were distinguished from viable cells by the incorporation of propidium iodide (PI; Sigma, St. Louis, MO). At 24 hr after the third stimulation, PI (final 10 μg/ml) was added to hippocampal slice cultures and incubated for a further 24 hr at 34°C. Slices exposed to kainic acid (KA; 100 μM) in the presence of PI for 24 hr served as the positive control in this assay. Two CA1 regions per slice were photographed with identical incident light intensity and exposure time with a fluorescence microscope (IX-50; Olympus, Tokyo, Japan) at 48 hr after the third stimulation. PI fluorescence intensity was measured on each micrograph in NIH Image software (Tominaga-Yoshino et al., 2002) and normalized by the background fluorescence acquired in the region not occupied by the slice.

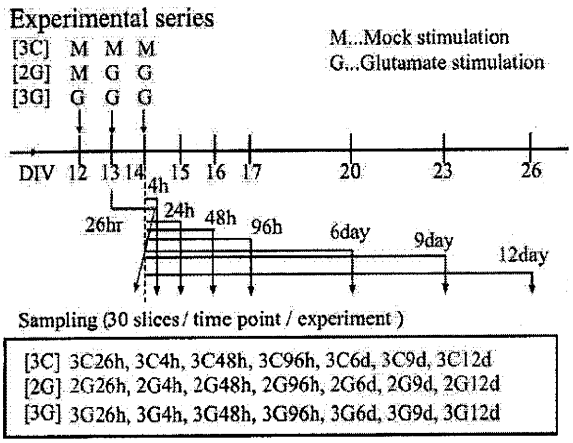

Fig. 1. Stimulation and sampling procedures. As described in Materials and Methods, hippocampal slices obtained from P8 rats were maintained in culture for 12d (DIV 12) before the start of the experiment to be stabilized both physically and physiologically. Slices were then stimulated in three ways ([3C], [2G], and [3G]) at 24-hr intervals on DIV12, 13, and 14. At each time point after the third stimulation, 30 each of the [3C], [2G], and [3G] slices were pooled (five slices × six wells) and used for RNA preparation. As a standard time point before the third stimulation, 26 hr after the second stimulation was used (26h). For protein extraction and Western blotting, 24 each of the slices stimulated in the three ways were pooled at 48 hr after the third stimulation.

Microarrays and Hybridization Conditions

Original oligonucleotide microarray was prepared as previously described (Takahashi et al., 2005). The contents of the synaptoarray are listed in Supporting Information Table I. A high-density microarray with oligonucleotide probes for 22,575 genes (rat oligoDNA microarray; Agilent Technologies, Palo Alto, CA) was used for screening genes differentially expressed by repetitive stimulation. Total RNA was prepared from pools of 30 similarly treated hippocampal slices using Trizol reagent (Invitrogen, Carlsbad, CA), reverse-transcribed with an oligo-dT primer containing the promoter sequence for T7 RNA polymerase, and amplified using RNA Transcript SureLABEL Core Kit (Takara Bio Inc., Shiga, Japan) with amino-allyl UTP incorporation. Amplified cRNA was purified with a QIAquick Nucleotide Removal Kit (Qiagen, Valencia, CA) and coupled either with cyanine 3 (Cy3; [3C] or [2G] slices) or with cyanine 5 (Cy5; [3G] slices). Labeled cRNA was purified with QIAquick Nucleotide Removal Kit (Qiagen) and fragmented using RNA Fragmentation Reagents (Ambion Diagnostics, Austin, TX). For one microarray, 1 μg each of Cy3- and Cy5-labeled samples to be compared was mixed in a final 500 μl of hybridization solution containing the following components at the following final concentrations; 0.02 μg/μl mouse Cot1-DNA (Invitrogen), 6 ng/μl oligo-dA 10mer (Sigma-Genosys, Hokkaidou, Japan), 0.3 μg/μl yeast tRNA (Invitrogen), 3.4× SSC, 0.3 ml/liter SDS (Gibco; 10 ml/liter SDS; DeRisi et al., 1996). The mixture was heated at 95°C for 1 min and clarified by centrifugation. Hybridization was performed in a hybridization chamber (Agilent Technologies) at 55°C for 16 hr with rotation (5 rpm). After hybridization, the chamber was disassembled in wash buffer I (6× SSC, 0.005 ml/liter Triton X-102), and the array slide was washed successively in wash buffer I for 10 min and wash buffer II (0.1× SSC, 0.005 ml/liter Triton X-102) for 5 min on ice and dried with N_2 gas.

Microarray Data Acquisition and Analysis

After hybridization, microarrays were scanned with DNAscope IV (GeneFocus Biomedical Photometrics Inc.). The fluorescence intensity signals from microarray images were quantified with ImaGene 5.5 (Biodiscovery, Los Angeles, CA) using the local background correction (GeneSight 3.5.2; Biodiscovery). The background-corrected Cy3 and Cy5 fluorescence intensity data from the synaptoarray were exported to Microsoft Excel and normalized using five internal standard genes (*rpL3, rpL13a, rpL22, rpL23, Ppia*) as described previously (Takahashi et al., 2005). Data from the high-density array were normalized by global normalization. Gene expression profiles were obtained from K-mean cluster analysis with software Gene Cluster (written by Michael Eisen, Stanford University).

Real-Time Quantitative Fluorescence-Based PCR

Expression levels of representative genes were quantified by fluorescence-based real-time PCR using the Smart Cycler System (Applied Cepheid) with Takara ExTaq (Takara Bio Inc.) and SYBR Green I (Molecular Probes, Eugene, OR) and were normalized with *rpl13a* as an internal standard. PCR primers (Table I) were designed in Oligo 6.0 primer analysis software (Molecular Biology Insights).

Western Blotting

Western blotting was performed as described previously (Kawaai et al., 2009). Briefly, PVDF membranes with proteins separated by SDS-PAGE were blocked with 5.0% skim milk in PBS containing 0.05% Tween-20 (PBST) for 1 hr and probed with the primary antibody for 1 hr at RT. The primary antibodies used were mouse anti-β-actin antibody (Sigma), rabbit anti-Syt4 antibody (IBL, Gunma, Japan), rabbit anti-mGluR5 antibody (Upstate, Lake Placid, NY), rabbit anti-BDNF antibody (N-20; Santa Cruz Biotechnology, Santa Cruz, CA), rabbit antiphospho-cofilin antibody (ab12866; Abcam, Tokyo, Japan), and rabbit anticofilin antibody (ab42824; Abcam). After being washed with PBST, the membranes were incubated with an appropriate HRP-conjugated secondary antibody, and signals were detected with Immobilon Western Detection Reagents (Millipore, Bedford, MA). A FujiFilm LAS4000 miniluminescent image analyzer was used to photograph the blots. Quantitative determination was performed with Multi Gauge (3.0; Fujifilm, Tokyo, Japan).

Immunostaining and Phalloidin Staining

Cultured hippocampal slices were washed once with PBS, fixed with 4.0% paraformaldehyde in PBS for 10 min, permeabilized with 1% Triton X-100 in PBS (PBS-Tx) for 5 min, and blocked with 1.0% skim milk with 1.0% normal goat serum (Vector Laboratories, Burlingame, CA) in PBS-Tx for 60 min at RT. Slices were then incubated with rabbit

TABLE I. Primers for Real-Time Quantitative PCR

	Forward	Reverse
bdnf	GGAGGCTAAGTGGAGCTGACATAC	GTGCTTCCGAGCCTTCCTTTAGG
syt4	AGTTTTGGATTCTGAAAGGGGATC	TTGTCTCCTGGGGAAGTCACAG
ania4	AACACTCCTTCATTACTTGCTTCC	AGTGGTTCCTTCTACAATGTTGAG
grm5	GCCCTCACTCCACCATCGCC	CTCTGCGTGTAATCTCTGATGATG
rgs2	GAAGTCCAGATGTGGTTCTGTTG	ATTCTTCACTTCTCAGGGCTGTC
ywhaz	CCATGCGGATCAAGCACAGCG	TAGCCGTCATCTCAAGTTATTTCC
slc6a12	GTGCTCCAGGAATCTGTTTGCC	AGCAGAGAGCAGCAAGTCCAAG
gabarapl2	TAGAGGGCTGAAGAGATGGCTC	AGGCAGGTAAGGGCATCAGATG
slc6a11	CCAAGGTCAAAGGCGACGGTAC	TTTACACGCAGGGAAGGAAGGC
cfl1	GCTGCCCTTTTCCTGCCAGAC	GGGATGGAGGGAAAAGGACGG
ssh11	CGACAGAAGGAGAAAGAACTGAG	GCTCATTTCGGATTTCCTTAGAAG
limk1	CATCTCTTCACTCTGCTTCAGTTG	CCTTGCCTCTTTCAGTCCTGGT
pak4	TGTGTCTCTATCTCAGCCTGGG	TAACTTGAGGGATTGGCGGCAG
casp3	CCCATAAGCCTCCTTATTGCAC	CACCACATGCTGTATTTACTTAG
rpl13a	GGAAGTACCAGGCAGTGACAGC	CTTGAGGACCTCTGTGAACTTGC

anti-Syt4 antibody (IBL) for 60 min at RT. After three washes with PBS for 15 min in total, Alexa 488-conjugated goat anti-rabbit IgG (Invitrogen) was applied for 60 min at RT. For phalloidin staining, Alexa 594-conjugated phalloidin (Invitrogen) was applied to fixed and permeabilized slices for 60 min at RT. After being washed with PBS, the coverslips were mounted with Vectashield (Vector Laboratories) and observed under a Nikon E-600 microscope (Nikon, Tokyo, Japan) for immunostaining. For phalloidin staining, the Z-projection images (2-μm step size, 15 sections, maximum intensity projection by FV1000 software) were obtained by confocal fluorescence microscopy (FV1000; Olympus, Tokyo, Japan). Quantitative determination was performed in ImageJ software (v1.42q; NIH).

Electron Microscopy

To prevent the destruction of actin microfilaments (Maupin-Szamier and Pollard, 1978), the slice was prepared as described by Mbassa et al. (1988) and Dinno and Mugnaini (2000), with minor modifications. Hippocampal slice cultures were fixed with 2% paraformaldehyde (PF) and 1.5% glutaraldehyde (GA) in 0.1 M phosphate buffer (PB) for 12 hr at 4°C, followed by washing in 0.1 M PB (3 × 5 min). These slices were rinsed in 50 mM maleate buffer (MB) at pH 6.0 for 5 min and incubated with phalloidin (10 mg/ml; Sigma), 1% tannic acid (TAAB, Berkshire, United Kingdom), and 5% dimethylsulfoxide (DMSO) in 50 mM MB, pH 6.0. After being washed in MB (3 × 5 min), the slices were stained en bloc in the dark at 4°C for 2 hr with 1% uranyl acetate in MB and washed again in the buffer for 3 × 5 min. In the subsequent steps, slices were dehydrated in a graded series of ethanol and infiltrated with Quetole 812 resin (Nissin-EM, Tokyo, Japan) at RT. Finally, embedded slices were cured at 60°C for 3–4 days. Ultarathin sections (80 nm thick) were stained with uranyl acetate and lead citrate and exmamined in JEM 1010 electron microscope (JEOL, Tokyo, Japan).

Statistical Analysis

Statistical comparison between two independent groups of data was performed with the Student's *t*-test. Statistically significant differences are denoted $*P < 0.05$, $**P < 0.01$, and $***P < 0.001$ in all the figures.

RESULTS

Time Course of Expression Changes in Synapse- and Cytoskeleton-Related Genes After Repetitive Glutamate Stimulation

Gene expression changes induced by repetitive stimulation were first monitored by comparing expression profiles of three times glutamate-stimulated slices ([3G] slices) with those of three times mock-stimulated slices ([3C] slices) using the custom oligonucleotide DNA microarray synaptoarray containing probes for ~300 genes mainly involved in the construction and functioning of synapses (Takahashi et al., 2005; Kitamura et al., 2007; a complete list of genes on the microarray is supplied as Supp. Info. Table I).

At each time point, RNA extracted from 30 each of [3C] and [3G] slices were compared by competitive hybridization. To reduce individual variations, slices obtained from each animal were equally divided between [3C] and [3G] preparations. Because our preliminary experiment showed that significant changes in gene expression profiles were not detected at 1 hr after the third stimulation (3G1h), seven time points between 4 hr and 12 days after the third stimulation (4 hr, 24 hr, 48 hr, 96 hr, 6 days, 9 days, 12 days) were selected for analysis together with 26 hr after the second stimulation as a standard time point before the third stimulation (Fig. 1).

From the results of competitive hybridization, genes showing more than 50% up- or down-regulation at least once during the experimental time course were selected for further analysis (total of 77 genes). By k-means clustering, these 77 genes were classified into four groups (I–IV) with typical expression profiles as shown in Figure 2A,B. Comparison of these expression profiles revealed that changes in gene expression after the third stimulation occurred in two phases, an early

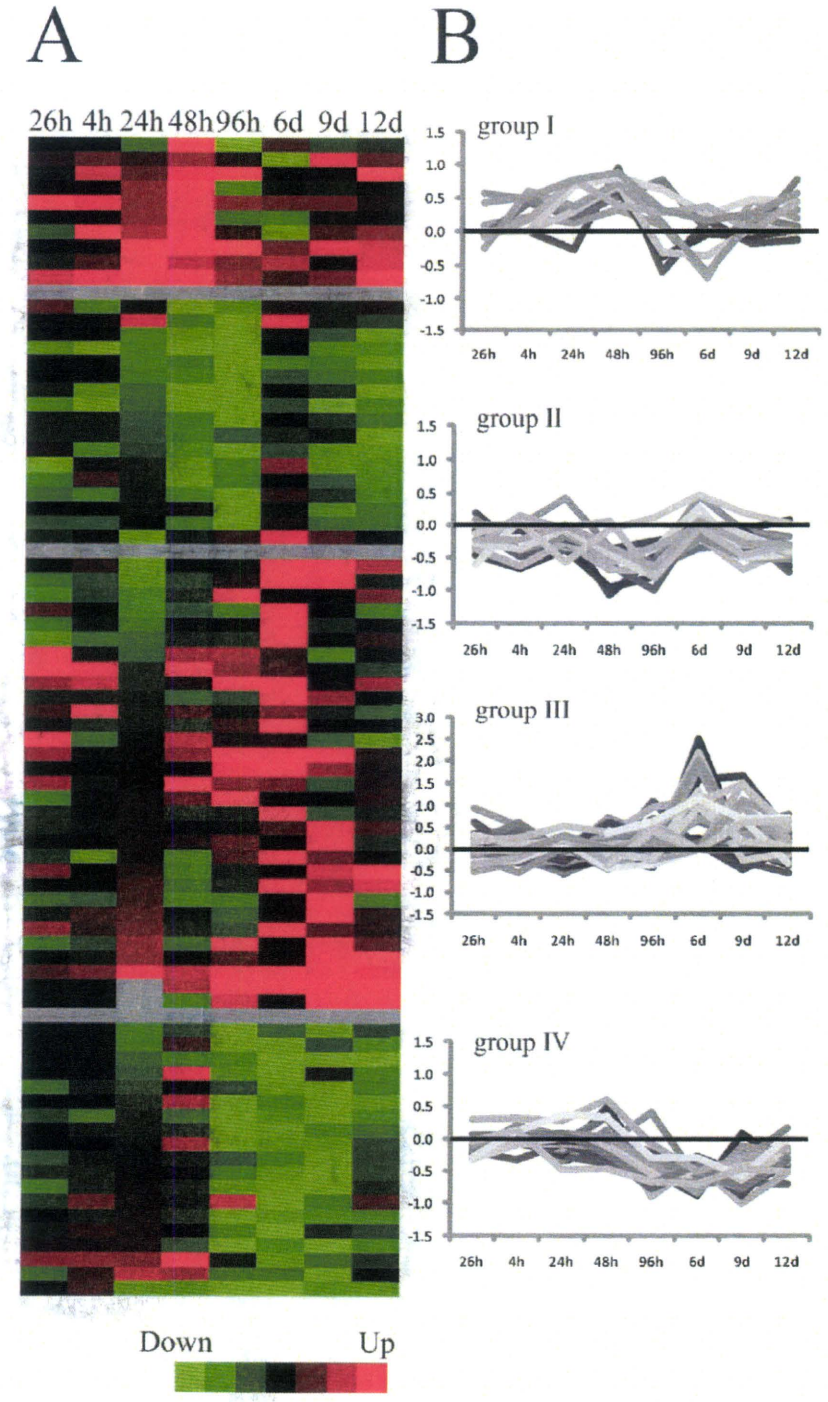

Fig. 2. Expression profiles of synapse- and cytoskeleton-related genes after repetitive stimulation. **A:** Classification of genes into four groups according to expression patterns by k-means clustering (k = 4). Genes showing more than 50% up-regulation (red) or down-regulation (green) in the three times glutamate-stimulated slices (3G) relative to mock-stimulated slices (3C) are colored. **B:** Time course of expression changes of individual genes in each group. For each gene, average expression ratios at each time point are expressed in logarithm of base 2 ($\log_2$ [3G]/[3C]) and plotted. Sampling time points between 4 hr and 12 days after the third stimulation are shown on the abscissa, with 26 hr representing the standard time point at 26 hr after the second stimulation.

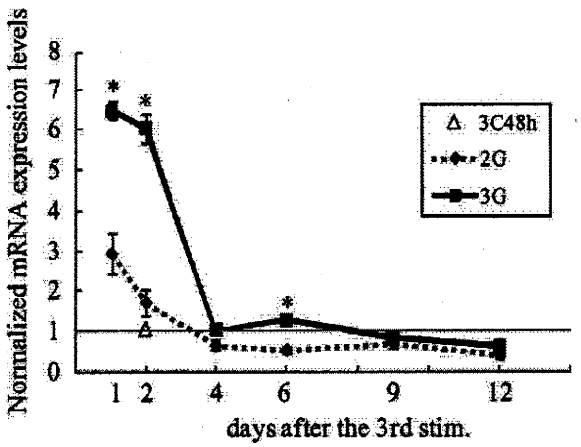

Fig. 3. Differences in the expression profiles of *bdnf* mRNA following two and three glutamate stimulations. Expression levels of *bdnf* mRNA in [2G] slices (lozenges) and [3G] slices (squares) at different time points after the last stimulation (day 0) were analyzed by real-time PCR using *rpL13a* as an internal standard and plotted relative to the level of *bdnf* mRNA in the control [3C] slices at 48 hr (triangle; mean ± SEM; n = 6, from two independent series of cultures).

phase (24 hr, 48 hr and 96 hr) and a late phase (6, 9, and 12 days). In the early phase, a peak of up-regulation was observed at 48 hr (group I), and the strongest down-regulation was observed at 48–96 hr (group II). In the late phase, significant up-regulation of group III genes was observed at 6–9 days. Group IV genes were persistently down-regulated between 96 hr and 9 days.

In the previous study, Tominaga-Yoshino et al. (2008) followed the course of synaptic enhancement after repetitive glutamate stimulation electrophysiologically and found that, after a decline of the initial enhancement of fEPSP (LTP) within 4 hr, there was a second and persistent enhancement of fEPSP (RISE) starting from 24 hr after the third stimulation and lasting for more than 3 weeks. An increase in the number of synaptic sites was also detected at 5 days after the third stimulation. Gene expression changes in the early phase may thus contribute primarily to the conversion from the transient LTP to the RISE.

Differences in the Expression Profiles of *bdnf* mRNA in Twice- and Thrice-Stimulated Slices

As one of the key factors regulating activity-dependent changes at the synapse, we compared expression profiles of *bdnf* mRNA in [2G] and [3G] slices by real-time PCR (Fig. 3). At 24 hr after the last stimulation, strong up-regulation of *bdnf* mRNA was observed in both [2G] and [3G] slices. Up-regulation in [3G] slices was much greater and persisted longer than that in [2G]slices. At 96 hr, *bdnf* expression in both types of slices was back to the baseline level. In [3G] slices, however, there was a small but significant second up-regulation at day 6. The earlier of the two phases of gene expression changes observed in Figure 2 thus corresponds to the first large peak of *bdnf* expression.

Comprehensive Screening of Gene Expression Changes 48 Hours After the Third Stimulation

From the time course analysis described above (Figs. 2, 3), we chose 48 hr after the third stimulation as a fixed time point at which to investigate thoroughly the genes responsible for the establishment of RISE using commercially available high-density arrays (Agilent Technologies). To make sure that the observed expression changes were not reflecting the apoptotic process induced by stimulation with high concentrations of glutamate in vitro (Schubert and Piasecki, 2001), histological evaluation of cell viability and analysis of caspase 3 (*casp3*) gene expression (Kroemer and Martin, 2005) were performed at this time point. As shown in Figure 4A, there was no significant difference in cell viability observed between slices experiencing three glutamate stimulations (3G48h) or three mock stimulations (3C48h), while slices exposed to 100 μM kainic acid for 24 hr exhibited significant incorporation of propidium iodide (PI), indicating cell death (Sakaguchi et al., 1997). Real-time PCR analysis further showed that the expression level of *casp3* in [3G] slices did not differ significantly from that of [3C] or [2G] slices (Fig. 4B). These data thus confirm that the glutamate stimulation protocol used in this study did not induce *casp3*-dependent apoptosis.

To increase efficiency and reliability of comprehensive screening, differentially stimulated slices were compared in two pairs by competitive hybridization 48 hr after the last stimulation, [3G] slices vs. [3C] slices and [3G] slices vs. [2G] slices. By focusing on differentially expressed genes detected in both pairs, genes progressively up- or down-regulated by repetitive stimulation and genes affected specifically by the third stimulation should be identified. Among the 22,575 gene probes on the high-density array, probes with signal intensities above 500 in both samples of the pair were selected for further analysis, and only probes showing consistent expression ratios of more than 1.2 (up-regulated) or less than 0.83 (down-regulated) were selected as differentially expressed. As a result, 1,437 up-regulated and 1,906 down-regulated probes were detected in the 3G vs. 3C comparison, whereas 1,136 up-regulated and 1,193 down-regulated probes were detected in the 3G /vs. 2G comparison (Supp. Info. Fig. 2A). Among these two pairs of comparisons, 701 up-regulated probes (3.1% of total probes) and 557 down-regulated probes (2.5%) were shared (Supp. Info. Fig. 2B), which were considered as candidate genes responding to repetitive stimulation.

We focused, among the candidate genes, on those up-regulated by more than two-fold in either pair of comparisons (3G/3C or 3G/2G), which amounted to 289. By deleting genes of unknown function, we finally ended up with a list of 176 putative repetitive stimula-

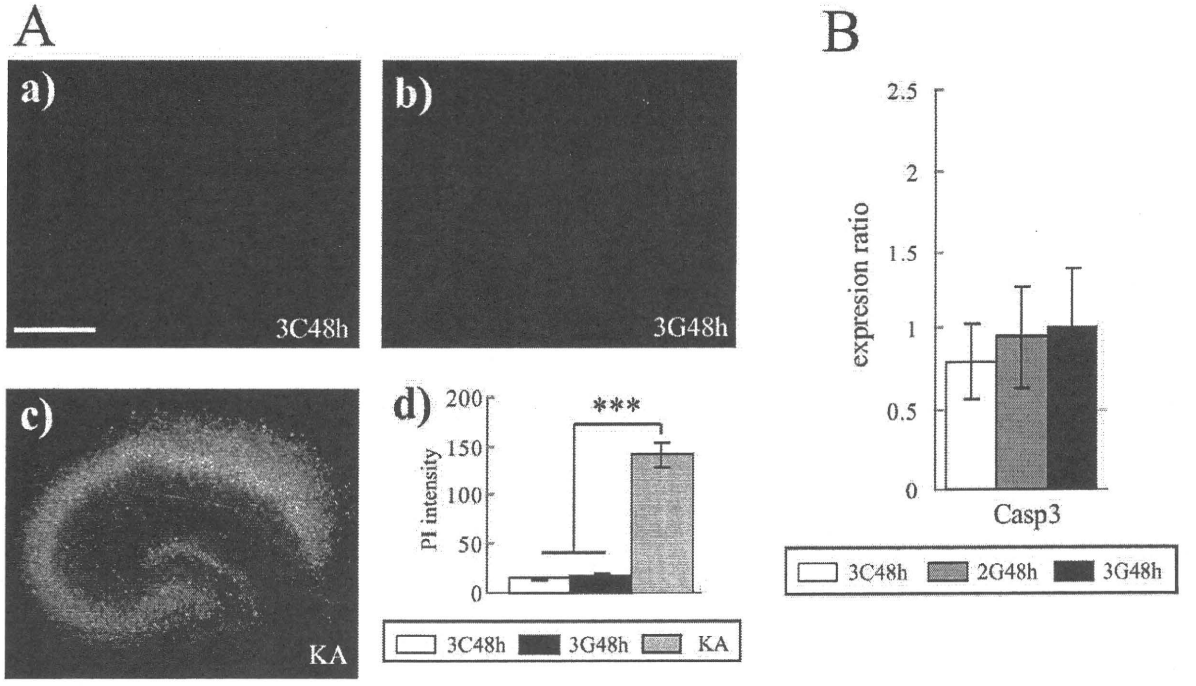

Fig. 4. Confirmation of cell viability after repetitive stimulation. **A:** Histochemical confirmation of cell viability by the absence of propidium iodide (PI) staining. Three times mock-stimulated ([3C]; a) or glutamate-stimulated ([3G]; b) hippocampal slices at 24 hr after the third stimulation were further incubated in culture medium containing 10 μg/ml PI for 24 hr at 34°C. A slice exposed to 100 μM kainic acid for 24 hr in the presence of PI is shown as a positive control (KA; c). In d, total PI fluorescence of each micrograph was quantified in NIH Image software (mean ± SEM; n = 3). **B:** Real-time quantitative PCR analysis of *casp3* in [3C], [2G], and [3G] slices at 48 hr after the last stimulation using *rpL13a* as an internal standard (mean ± SEM; n = 6, from two independent series of cultures). Scale bar = 500 μm.

tion-induced genes (provided as Supp. Info. Table III). Several genes previously reported to be induced by physiological/unphysiological stimuli or behavioral conditionings and to be correlated with synaptic plasticity and memory were found on this list; *grm5* (type 1 metabotropic glutamate receptor 5; Manahan-Vaughan et al., 2003), *rgs2* (regulator of G-protein signaling; Ingi et al., 1998), *syt4* (synaptotagmin-4; Vician et al., 1995), and *ania4/carp/dclk1* (doublecortin-like kinase 1; Berke et al., 1998; Vreugdenhil et al., 1999). Though not as highly up-regulated as those on the list, three other genes known to be activity-induced were also included in the 701 candidate up-regulated genes, *bdnf* (brain-derived neurotrophic factor; Hall et al., 2000), *cpg1* (candidate plasticity-related gene 1; Nedivi et al., 1993), and *rheb* (rapidly and transiently induced gene in hippocampal granule cells; Yamagata et al., 1994). In addition to these activity-related genes, *ywhaz/14-3-3ζ* (tyrosine 3-monooxygenase/tryptophan 5-monooxygenase activation protein, zeta polypeptide) involved in the regulation of actin dynamics (Soosairajah et al., 2005) and *slc6a11* (neurotransmitter transporter, GABA, member 11) were among the 176 highly up-regulated genes.

To confirm microarray data, real-time quantitative PCR analysis was performed with the six representative highly up-regulated genes mentioned above (*grm5, rgs2, syt4, ania4, ywhaz, slc6a11*) as well as the following two related genes, which were among the 701 up-regulated candidate genes; *slc6a12* (neurotransmitter transporter, betaine/GABA, member 12), and *gabarapl2* ($GABA_A$ receptor-associated protein-like 2). Expression ratios of [3G] and [2G] slices relative to [3C] slices at 48 hr after the last stimulation were obtained using *rpL13a* (60S ribosomal subunit protein gene) as internal stnadard, yielding results mostly consistent with microarray data (Fig. 5). Compared with the twice-stimulated sample, significant up-regulation by the third stimulation was observed with *syt4, ywhaz, slc6a12*, and *gabarapl2*. It is also noteworthy that *ania4, grm5*, and *syt4*, which have been reported to be induced by extensive stimulation (e.g., seizure), were up-regulated by repeating the weaker stimulation three times without induction of apoptosis (Fig. 4).

Increases in the Protein Levels of BDNF, GRM5, and SYT4 by Repetitive Glutamate Stimulation

We confirmed the expression of three repetitive stimulation-induced genes, *bdnf, grm5*, and *syt4*, at the protein level. As shown in Figure 6A, BDNF and mGluR5 proteins were increased both in [2G48h] slices

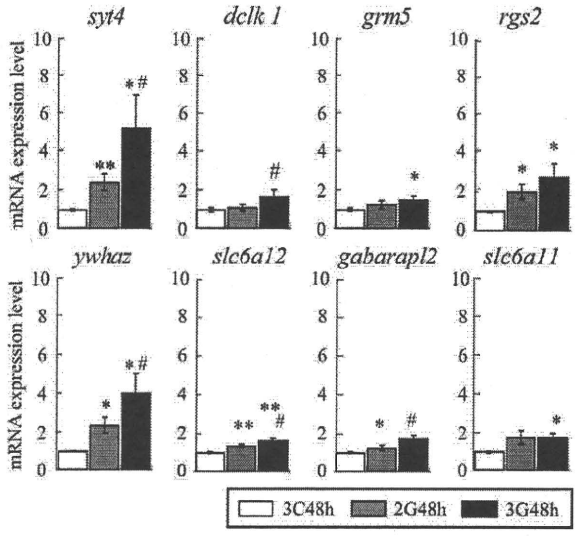

Fig. 5. Real-time quantitative PCR analysis of the representative genes. Repetitive stimulation-dependent changes in the expression of eight representative genes detected by microarray analyses were validated by real-time quantitative PCR. For each gene, average expression ratios of [2G] and [3G] slices relative to [3C] slices at 48 hr after the last stimulation (3G48h/3C48h or 2G48h/3C48h) are shown. All expression ratios were normalized with that of *rpL13a* as internal standard (mean ratio ± SEM; n = 6, from two independent series of cultures). Values with statistically significant differences compared with that of [3C] slices are marked $^{*}P < 0.05$ or $^{**}P < 0.01$, and those of [3G] slices compared with that of the [2G] slices are marked $^{\#}P < 0.05$.

and in [3G48h] slices, whereas Syt4 protein was increased only in [3G48h] slices. The third stimulation-specific increase of Syt4 was further confirmed by immunostaining the hippocampal slices with anti-Syt4 antibody as shown in Figure 6B. Consistent with the results of Western blotting, Syt4 immunoreactivity was significantly increased in [3G] slices compared with [3C] and [2G] slices. It is notable that the up-regulation of Syt4 was most prominent in the CA3 region, where it was localized to perikarya of pyaramidal neurons. Immunostaining at different time intervals after the third stimulation revealed that Syt4 was also up-regulated at 24 hr and 96 hr, but not at later time points of 6 days, 8 days, and 12 days (data not shown).

Coordinated Changes in the Expression of Genes Regulating Cofilin Phosphorylation Leading to Changes in Actin Polymerization

Because *ywhaz/14-3-3ζ* is known as a regulator of *ssh1l* (slingshot homolog 1) phosphatase that activates the actin depolymerizing factor cofilin, and cofilin was among the genes in group IV (Fig. 2), we investigated by real-time quantitative PCR the effect of repetitive stimulation on the expression of four additional genes involved in this pathway (Fig. 7A), *ssh1l, pak4* (p21 (CDKN1A)-activated kinase 4), *limk1* (LIM-domain containing protein kinase 1), and *cfl1* (cofilin 1, non-muscle). Although probes for these four genes were on the high-density array, sufficient signal intensities were not obtained.

Cofilin serves as one of the major stimulators of actin turnover and actin filament dynamics by enhancing depolymerization at the minus end and by severing actin filaments to produce new plus ends. Cofilin is inactivated through phosphorylation of the N-terminal Ser3 by LIMK1 and reactivated through dephosphorylation by SSH1. Activities of both of these enzymes are regulated through phosphorylation by PAK4, which activates LIMK1 and inactivates SSH1. Ywhaz, on the other hand, inhibits SSH1 activity by sequestering it in the cytoplasm. As summarized in Figure 7B, transcription of genes for all of these five proteins were up-regulated compared with control (3C) 48 hr after the second stimulation (2G), indicating that glutamate stimulation activated actin filament dynamics by up-regulating factors involved in both polymerization and depolymerization. In contrast, these genes were differentially affected by the third stimulation; *cfl1* and *ssh1l* were down-regulated, whereas *pak4, ywhaz*, and *limk1* were further up-regulated. This should lead to suppression of actin filament dynamics and enhancement of actin polymerization through cofilin phosphorylation as summarized in Figure 7B.

To confirm the involvement of cofilin phosphorylation in the third-stimulation-specific RISE phenomenon, we examined the phosphorylation states of cofilin by Western blotting using the phosphorylated cofilin-specific antibody (Fig. 7C). Consistent with the expression profiles of actin dynamics regulators, the phosphorylation level of cofilin was significantly reduced after the second stimulation (2G48h) compared with the control (3C48h). Conversely, the phosphorylation level of cofilin showed a tendency to increase after the third stimulation (3G48h) compared with 2G48h. Estimation of the level of actin polymerization with fluorescently labeled phalloidin revealed that, consistent with changes in cofilin phosphorylation states, phalloidin staining was significantly decreased after the second stimulation (2G48h) compared with the control (3C48h) especially in the CA1 region (Fig. 7D). Conversely, intensity of phalloidin staining after the third stimulation (3G48h) was increased compared with 2G48h. In addition, direct observation of actin-containing filament structures in these slices by transmission electron microscopy after actin filament stabilization with phalloidin and tannic acid revealed an increase in the density of the 7–8-nm microfilament structures spreading from PSD and constructing the subsynaptic web in 3G48h slices compared with 2G48h slices (Fig. 7E). The results thus indicate that the second stimulation transiently destabilized the actin cytoskeleton, whereas the third stimulation suppressed actin filament dynamics and enhanced actin polymerization.

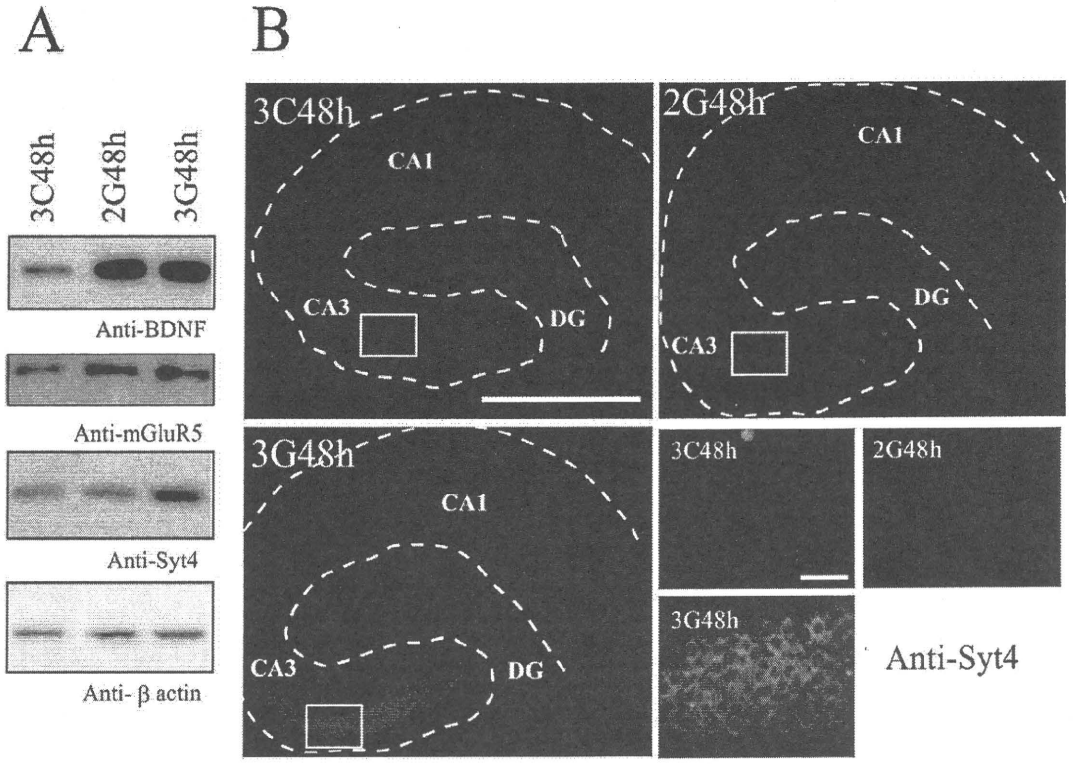

Fig. 6. **A,B:** Increases in the protein levels of BDNF, mGluR5, and Syt4 by repetitive glutamate stimulation. The lysate of the [3C], [2G], or [3G] slices obtained 48 hr after the last stimulation was analyzed by Western blotting with the antibodies against BDNF, mGluR5, Syt4, or β-actin as indicated. The [3C], [2G], and [3G] hippocampal slices 48 hr after the last stimulation were immunostained with anti-Syt4 antibody. The dashed line indicates the edge of the slice. Boxed regions are shown at higher magnification at the lower right corner. Scale bars = 500 μm in larger panels; 50 μm in smaller panels.

DISCUSSION

Correlations Among Genes Induced by Repetitive Stimulation, LTP, and Epileptic Activity

Because RISE develops after the repeated induction of LTP, several genes previously reported to be up-regulated during LTP induction in vitro or in vivo were detected among genes up-regulated by repetitive stimulation, as expected: *bdnf*, which has been shown to increase by the stimulus paradigm inducing LTP in CA1 in vitro and by contextual learning in vivo (Hall et al., 2000); *rgs2* (regulator of G protein signaling 2); and *grm5* (type1 metabotropic glutamate receptor 5) were induced following LTP induction in DG and CA1 in vivo (Manahan-Vaughan et al., 2003). In particular, larger and longer-lasting up-regulation by three repetitive stimulations compared with two was observed with *bdnf*, which has been shown to be a key factor in activity-dependent synaptic enhancement.

Furthermore, two genes reported to be induced in the hippocampus by kainate-elicited seizures were also up-regulated by repetitive stimulation; *ania 4/dclk 1* (Vreugdenhil et al., 1999) and *syt4* (Vician et al., 1995). *ania 4/dclk 1* Encodes a protein kinase similar to Ca^{2+}/calmodulin-dependent kinases (CAMK) but with an additional N-terminal doublecortin (DCX) homology domain. As with DCX, DCLK1 shows microtubule-binding and polymerization activities (Lin et al., 2000), suggesting that it may regulate neurite extension and cell migration. Syt4, on the other hand, has been shown recently to be localized to BDNF-containing vesicles and to regulate BDNF release negatively in response to synaptic activity (Dean et al., 2009). Such regulation by Syt4 may be a mechanism to avoid exhaustive stimulation and maintain the level of BDNF as well as synaptic strength in a useful range during long-lasting LTP. In contrast to kainate-induced seizures, which resulted in strong up-regulation of Syt4 protein in CA1, CA3, and DG in vivo (Vician et al., 1995), repetitive glutamate stimulation induced prominent up-regulation only in the CA3 region (Fig. 6B). The repetitive glutamate stimulation protocol used in this study thus achieved induction of genes that are dependent on stronger or nonphysiological stimuli without induction of excitotoxic cell death (Fig. 4). Insofar as epileptic seizures have also been reported to up-regulate *bdnf* (Kokaia et al., 1994; Poulsen et al., 2004), results of the present study indicate that the long-lasting synaptic enhancement induced by repet-

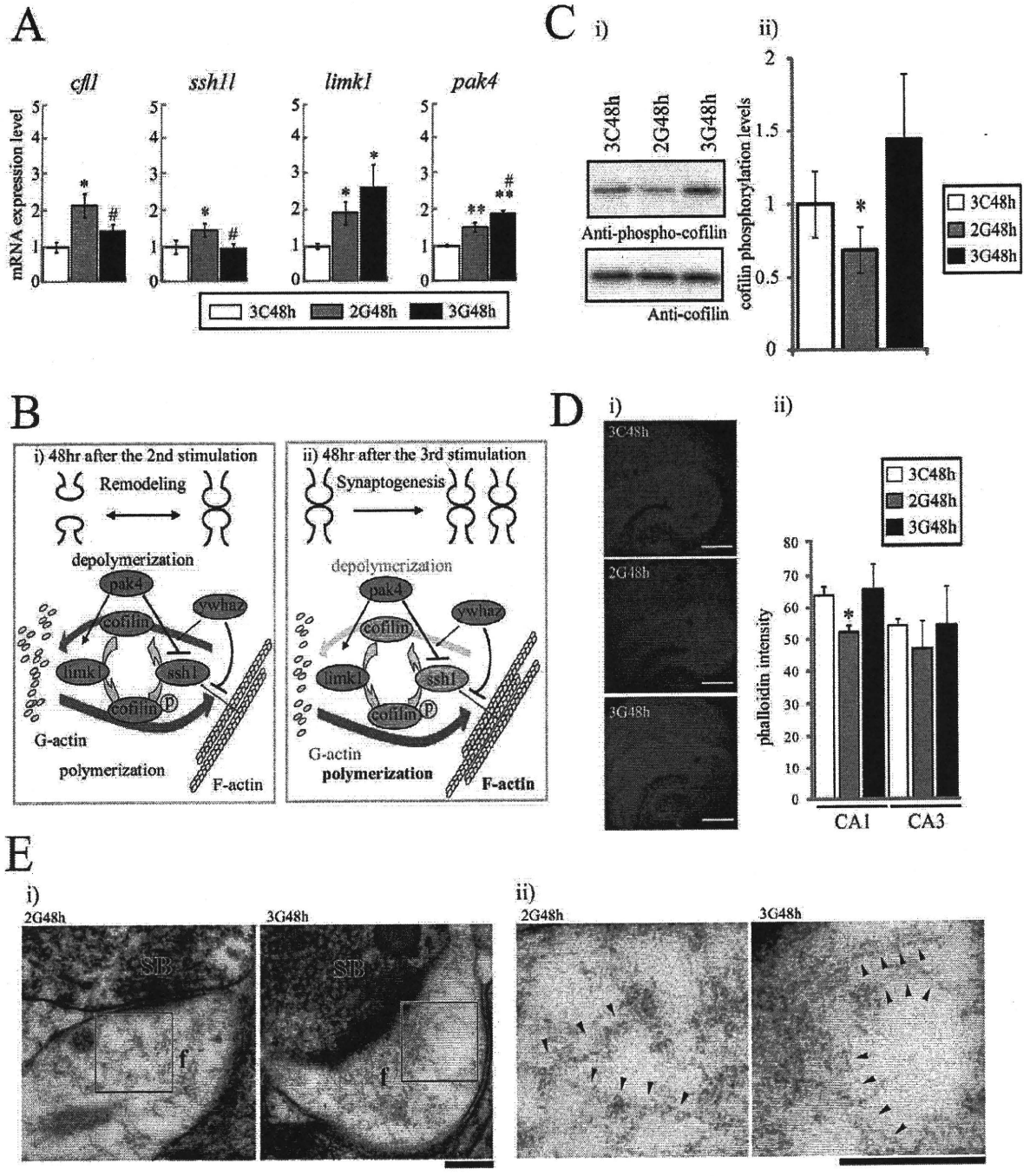

Fig. 7. Expression changes of genes involved in the regulation of actin dynamics by repetitive stimulation. **A:** Real-time PCR analysis of the differences in the expression of an additional four genes involved in the regulation of actin dynamics. For each gene, average expression ratios of [2G] and [3G] slices relative to [3C] slices at 48 hr after the last stimulation are shown (mean ± SEM; n = 6, from two independent series of cultures). All expression ratios were normalized with that of *rpL13a*. Values with statistically significant differences compared with the [3C] slices are marked $*P < 0.05$ or $**P < 0.01$, and those of [3G] slices compared with that of [2G] slices are marked $^{\#}P < 0.05$). **B:** Schematic representation of the regulation of actin filament dynamics after repetitive stimulation showing stimulatory (arrows) and inhibitory (blocked lines) interactions among the five genes. i) After two stimulations, five genes regulating actin dynamics were all up-regulated, indicating that both polymerization and depolymerization of actin were enhanced. ii) Three stimulations coordinately changed the expression of five genes to suppress actin depolymerization and enhance polymerization (cfl1 and SSH1 were down-regulated; PAK4, Ywhaz, and LIMK1 were up-regulated). **C:** i) Phosphorylation level of cofilin protein was analyzed by Western blotting with the antibodies against phosphophorylated cofilin (at Ser 3) and total cofilin as indicated. ii) Phosphorylation levels of cofilin were quantified by the ratio of phosphorylated-cofilin to total cofilin (mean ± SEM; n = 4). Values with statistically significant differences compared with [3C] slices are marked $*P < 0.05$. **D:** i) The [3C], [2G], and [3G] hippocampal slices 48 hr after the last stimulation were stained with Alexa 594-conjugated phalloidin selective for F-actin. ii) Relative intensities of fluorescent phalloidin staining in CA1 and CA3 regions of [3C], [2G], and [3G] slices 48 hr after the last stimulation. Values with statistically significant differences compared with [3C] slices are marked $*P < 0.05$. **E:** Electron microscopic analysis confirms the increase in the actin filament structures after repeated glutamate exposures. i) The 7–8-nm microfilaments spread from PSD and constructed subsynaptic web (f). Boxed areas in i are enlarged in ii. SB indicates presynaptic bouton. Arrowheads in ii indicate thin microfilaments extending from the web. Scale bars = 300 μm in D; 200 nm in E.

itive glutamate stimulation at least partially shares the common pathways leading to LTP and epileptic activity.

Effect of Repetitive Stimulation on GABAergic Neurotransmission

In addition to the positive modulations of excitatory synapses, negative modulations of inhibitory synapses have been shown to contribute to the induction of LTP (Casasola et al., 2004; Fiumelli et al., 2005). In our comprehensive screening, three genes involved in GABAergic neurotransmission were found to be up-regulated by repetitive glutamate stimulation; GABA transporters *slc6a12* and *slc6a11* and GABA receptor-interacting protein *gabarapl2* (Fig. 5). Up-regulation of GABA transporters may attenuate the inhibitory action of GABA by reducing its synaptic concentration.

The inhibitory nature of GABAergic transmission depends on the transmembrane Cl^- gradient, which is regulated mainly by the neuron-specific K^+-Cl^- cotransporter KCC2 responsible for Cl^- extrusion. A positive shift in the Cl^- reversal potential through activity-dependent suppression of KCC2 function (Fiumelli et al., 2005) as well as its gene expression (Rivera et al., 2004) is thus considered as one of the major mechanisms of activity-induced negative modification in inhibitory synapses. In our microarray analysis, *Slc12a5/KCC2* was found to be down-regulated to a similar degree after the second and the third stimulations (data not shown).

Kleschevnikov et al. (2004) have shown that the high-frequency stimulation (HFS) inducing LTP under normal conditions produced epileptiform activity in the presence of $GABA_A$ receptor antagonist picrotoxin (Kleschevnikov et al., 2004). A shift in the balance between excitatory and inhibitory pathways through attenuation of GABAergic neurotransmission may thus be another common basis for the induction of LTP, epileptic activity, and long-lasting synaptic enhancement by repetitive stimulation.

Modulation of Actin Filament Dynamics Leading to Structural Reorganization

Previous studies have shown that stimulation paradigms inducing LTP are associated with reorganization of the actin cytoskeleton characterized by an increase in filamentous actin (F-actin) content within dendritic spines (Fukazawa et al., 2003). In most cases, these changes were temporary and accomplished by the modification or translocation of the proteins associated with the actin cytoskeleton. In our time course analysis, however, numerous genes involved in the regulation of the actin cytoskeleton were found to change expression levels during the early phase after stimulation. In particular, five genes modulating the dynamics of actin polymerization through the cofilin pathway were found to be coordinately but differentially regulated at 48 hr after the second and the third stimulations (Figs. 5, 7); all five genes were up-regulated after the second stimulation, whereas *cfl1* and *ssh1l* were down-regulated and *ywhaz/14-3-3ζ*, *pak4*, and *limk1* were up-regulated after the third stimulation. Cofilin 1 is an actin-depolymerizing factor, which increases actin dynamics by severing actin filaments and binding to the severed plus ends. Cofilin1 is inactivated by LIM-kinase 1 through phosphorylation at Ser-3 and is reactivated by the phosphatase slingshot 1L, which, in turn, is inhibited by the kinase PAK4 and the ywhaz protein (Nagata-Ohashi et al., 2004). On the other hand, PAK4 kinase activates LIMK1 to regulate cooperatively the phosphorylation state of cofilin1 (Soosairajah et al., 2005). The observed expression changes in these genes after the second stimulation enhance actin dynamics by enhancing both polymerization and depolymerization, whereas changes after the third stimulation coordinately decrease the activity of cfl1 to slow actin dynamics and stabilize F-actin. Consistent with the gene expression profiles of actin dynamics regulators, cofilin phosphorylation and intensity of phalloidin staining (F-actin) were significantly reduced after the second stimulation compared with the control (3C48h). Conversely, cofilin phosphorylation, intensity of phalloidin staining, and actin microfilament structures were increased after the third stimulation compared with 2G48h (Fig. 7). These results thus indicate that stabilization of actin dynamics through cofilin phosphorylation underlies the structural reorganization leading to the establishment of RISE, the repetitive stimulation-induced long-lasting synaptic enhancement.

ACKNOWLEDGMENTS

The authors thank Mr. Tomoyuki Amemiya (RIKEN) for his assistance in the development of the DNA microarray; Dr. Masaki Takahashi (Aoyama Gakuin University) for valuable suggestions and help in microarray analysis during the initial phase of the study; and Dr. Takayuki Negishi, Ms. Madoka Inoue, and Mr. Hajime Shirane (Aoyama Gakuin University) for their assistance in designing primers for real-time quantitative PCR.

REFERENCES

Bear MF, Connors BW, Paradiso MA. 2001. Neuroscience: exploring the brain, 2nd ed. Baltimore: Lippincott Williams & Wilkins.

Berke JD, Paletzki RF, Aronson GJ, Hyman SE, Gerfen CR. 1998. A complex program of striatal gene expression induced by dopaminergic stimulation. J Neurosci 18:5301–5310.

Casasola C, Montiel T, Calixto E, Brailowsky S. 2004. Hyperexcitability induced by GABA withdrawal facilitates hippocampal long-term potentiation. Neuroscience 126:163–171.

Collingridge GL, Isaac JT, Wang YT. 2004. Receptor trafficking and synaptic plasticity. Nat Rev Neurosci 5:952–962.

Dean C, Liu H, Mark Dunning F, Chang PY, Jackson MB, Chapman ER. 2009. Synaptotagmin-IV modulates synaptic function and long-term potentiation by regulating BDNF release. Nat Neurosci (in press).

DeRisi J, Penland L, Brown PO, Bittner ML, Meltzer PS, Ray M, Chen Y, Su YA, Trent JM. 1996. Use of a cDNA microarray to analyse gene expression patterns in human cancer. Nat Genet 14:457–460.

Dino MR, Mugnaini E. 2000. Postsynaptic actin filaments at the giant mossy fiber-unipolar brush cell synapse. Synapse 38:499–510.

Fiumelli H, Cancedda L, Poo MM. 2005. Modulation of GABAergic transmission by activity via postsynaptic Ca^{2+}-dependent regulation of KCC2 function. Neuron 48:773–786.

Frey U, Frey S, Schollmeier F, Krug M. 1996. Influence of actinomycin D, a RNA synthesis inhibitor, on long-term potentiation in rat hippocampal neurons in vivo and in vitro. J Physiol 490:703–711.

Fukazawa Y, Saitoh Y, Ozawa F, Ohta Y, Mizuno K, Inokuchi K. 2003. Hippocampal LTP is accompanied by enhanced F-actin content within the dendritic spine that is essential for late LTP maintenance in vivo. Neuron 38:447–460.

Gahwiler BH, Capogna M, Debanne D, McKinney RA, Thompson SM. 1997. Organotypic slice cultures: a technique has come of age. Trends Neurosci 20:471–477.

Hall J, Thomas KL, Everitt BJ. 2000. Rapid and selective induction of BDNF expression in the hippocampus during contextual learning. Nat Neurosci 3:533–535.

Ingi T, Krumins AM, Chidiac P, Brothers GM, Chung S, Snow BE, Barnes CA, Lanahan AA, Siderovski DP, Ross EM, Gilman AG, Worley PF. 1998. Dynamic regulation of RGS2 suggests a novel mechanism in G-protein signaling and neuronal plasticity. J Neurosci 18:7178–7188.

Kawaai K, Hisatsune C, Kuroda Y, Mizutani A, Tashiro T, Mikoshiba K. 2009. 80K-H interacts with inositol 1,4,5-trisphosphate (IP3) receptors and regulates IP3-induced calcium release activity. J Biol Chem 284:372–380.

Kitamura C, Takahashi M, Kondoh Y, Tashiro H, Tashiro T. 2007. Identification of synaptic activity-dependent genes by exposure of cultured cortical neurons to tetrodotoxin followed by its withdrawal. J Neurosci Res 85:2385–2399.

Klann E, Dever TE. 2004. Biochemical mechanisms for translational regulation in synaptic plasticity. Nat Rev Neurosci 5:931–942.

Kleschevnikov AM, Belichenko PV, Villar AJ, Epstein CJ, Malenka RC, Mobley WC. 2004. Hippocampal long-term potentiation suppressed by increased inhibition in the Ts65Dn mouse, a genetic model of Down syndrome. J Neurosci 24:8153–8160.

Kokaia Z, Metsis M, Kokaia M, Bengzon J, Elmer E, Smith ML, Timmusk T, Siesjo BK, Persson H, Lindvall O. 1994. Brain insults in rats induce increased expression of the BDNF gene through differential use of multiple promoters. Eur J Neurosci 6:587–596.

Kroemer G, Martin SJ. 2005. Caspase-independent cell death. Nat Med 11:725–730.

Lin PT, Gleeson JG, Corbo JC, Flanagan L, Walsh CA. 2000. DCAMKL1 encodes a protein kinase with homology to doublecortin that regulates microtubule polymerization. J Neurosci 20:9152–9161.

Lisman J, Schulman H, Cline H. 2002. The molecular basis of CaMKII function in synaptic and behavioural memory. Nat Rev Neurosci 3:175–190.

Lynch MA. 2004. Long-term potentiation and memory. Physiol Rev 84:87–136.

Manahan-Vaughan D, Ngomba RT, Storto M, Kulla A, Catania MV, Chiechio S, Rampello L, Passarelli F, Capece A, Reymann KG, Nicoletti F. 2003. An increased expression of the mGlu5 receptor protein following LTP induction at the perforant path-dentate gyrus synapse in freely moving rats. Neuropharmacology 44:17–25.

Maupin-Szamier P, Pollard TD. 1978. Actin filament destruction by osmium tetroxide. J Cell Biol 77:837–852.

Mbassa G, Elger M, Kriz W. 1988. The ultrastructural organization of the basement membrane of Bowman's capsule in the rat renal corpuscle. Cell Tissue Res 253:151–163.

Muller D, Buchs PA, Stoppini L. 1993. Time course of synaptic development in hippocampal organotypic cultures. Brain Res Dev Brain Res 71:93–100.

Nagata-Ohashi K, Ohta Y, Goto K, Chiba S, Mori R, Nishita M, Ohashi K, Kousaka K, Iwamatsu A, Niwa R, Uemura T, Mizuno K. 2004. A pathway of neuregulin-induced activation of cofilin-phosphatase Slingshot and cofilin in lamellipodia. J Cell Biol 165:465–471.

Nedivi E, Hevroni D, Naot D, Israeli D, Citri Y. 1993. Numerous candidate plasticity-related genes revealed by differential cDNA cloning. Nature 363:718–722.

Otani S, Marshall CJ, Tate WP, Goddard GV, Abraham WC. 1989. Maintenance of long-term potentiation in rat dentate gyrus requires protein synthesis but not messenger RNA synthesis immediately post-tetanization. Neuroscience 28:519–526.

Poulsen FR, Lauterborn J, Zimmer J, Gall CM. 2004. Differential expression of brain-derived neurotrophic factor transcripts after pilocarpine-induced seizure-like activity is related to mode of Ca^{2+} entry. Neuroscience 126:665–676.

Rivera C, Voipio J, Thomas-Crusells J, Li H, Emri Z, Sipila S, Payne JA, Minichiello L, Saarma M, Kaila K. 2004. Mechanism of activity-dependent downregulation of the neuron-specific K-Cl cotransporter KCC2. J Neurosci 24:4683–4691.

Sakaguchi T, Okada M, Kuno M, Kawasaki K. 1997. Dual mode of N-methyl-D-aspartate-induced neuronal death in hippocampal slice cultures in relation to N-methyl-D-aspartate receptor properties. Neuroscience 76:411–423.

Schubert D, Piasecki D. 2001. Oxidative glutamate toxicity can be a component of the excitotoxicity cascade. J Neurosci 21:7455–7462.

Shinoda Y, Tominaga-Yoshino K, Ogura A. 2003. The dendritic layer-specific persistent enhancement of synaptic transmission induced by repetitive activation of protein kinase A. Neurosci Res 47:191–200.

Soosairajah J, Maiti S, Wiggan O, Sarmiere P, Moussi N, Sarcevic B, Sampath R, Bamburg JR, Bernard O. 2005. Interplay between components of a novel LIM kinase-slingshot phosphatase complex regulates cofilin. EMBO J 24:473–486.

Steward O, Schuman EM. 2001. Protein synthesis at synaptic sites on dendrites. Annu Rev Neurosci 24:299–325.

Takahashi M, Kondoh Y, Tashiro H, Koibuchi N, Kuroda Y, Tashiro T. 2005. Monitoring synaptogenesis in the developing mouse cerebellum with an original oligonucleotide microarray. J Neurosci Res 80:777–788.

Tominaga-Yoshino K, Kondo S, Tamotsu S, Ogura A. 2002. Repetitive activation of protein kinase A induces slow and persistent potentiation associated with synaptogenesis in cultured hippocampus. Neurosci Res 44:357–367.

Tominaga-Yoshino K, Urakubo T, Okada M, Matsuda H, Ogura A. 2008. Repetitive induction of late-phase LTP produces long-lasting synaptic enhancement accompanied by synaptogenesis in cultured hippocampal slices. Hippocampus 18:281–293.

Urakubo T, Ogura A, Tominaga-Yoshino K. 2006. Ultrastructural features of hippocampal CA1 synapses with respect to synaptic enhancement following repeated PKA activation. Neurosci Lett 407:1–5.

Vician L, Lim IK, Ferguson G, Tocco G, Baudry M, Herschman HR. 1995. Synaptotagmin IV is an immediate early gene induced by depolarization in PC12 cells and in brain. Proc Natl Acad Sci U S A 92:2164–2168.

Vreugdenhil E, Datson N, Engels B, de Jong J, van Koningsbruggen S, Schaaf M, de Kloet ER. 1999. Kainate-elicited seizures induce mRNA encoding a CaMK-related peptide: a putative modulator of kinase activity in rat hippocampus. J Neurobiol 39:41–50.

Yamagata K, Sanders LK, Kaufmann WE, Yee W, Barnes CA, Nathans D, Worley PF. 1994. rheb, A growth factor- and synaptic activity-regulated gene, encodes a novel Ras-related protein. J Biol Chem 269:16333–16339.